High Frame Rate Electrical Impedance Tomography System for Monitoring of Regional Lung Ventilation

Mohamad Rahal, Jiang Dai *Senior Member, IEEE*, Yu Wu, Andy Bardill, Richard Bayford, *Life Senior Member, IEEE* and Andreas Demosthenous, *Fellow, IEEE*

***Abstract*— This paper describes the development of a compact high frame rate passive electrical impedance tomography system. The injected current amplitude and frequency can be adjusted to fit any EIT application. Measured results show that the system is capable of high frame rate of 89 fps and has power consumption of 1.7 W. It has automatic gain control that reduces noise and improves the quality of the measured EIT image. A comparison is made with other EIT systems to show the potential of the developed system.**

***Clinical Relevance*— The developed EIT system has application in the clinical assessment of neonatal and SARS-CoV-2 patients. In these applications, there is an urgent need for a low cost, bedside, non-invasive imaging system, to continuously monitor dynamic changes in regional lung ventilation.**

I. Introduction

Electrical impedance tomography (EIT) is a technique used in biomedical applications, for regional lung monitoring and ventilation [1], and brain imaging [2]. EIT has the potential to be a very useful tool for the monitoring of lung ventilation of SARS-CoV-2 patients. In this application, there is difficulty in applying traditional imaging techniques such as X-ray and magnetic resonance imaging (MRI) on very sick patients in intensive care units (ICUs). Although EIT suffers from poor resolution compared to traditional imaging techniques, it has advantages in that it is simple, cost-effective, non-invasive, does not use ionizing radiation, and has high temporal resolution. EIT is a technique that images the changes in the admittance or impedance distribution of the living tissues because of current injection using surface electrodes as depicted in Fig. 1. In a typical EIT application, a small alternating current (AC) of about 1 mA at few hundred kHz is commonly injected through one electrode pair and voltage differences are recorded from the remaining electrodes. Then, the current is injected using the next pair of electrodes until all the available electrodes have been switched. The switching speed determines the frame rate, with real time imaging requiring frame rates from a few Hz up to 50 Hz. For example, in neonatal applications there is a need for a high frame rate as the breathing rate of neonates is higher compared to adults. Using the collected frames and the application of inverse problem algorithms, estimates of resistivity distribution can be obtained. The number of electrodes applied varies depending on the application, with the number being restricted to 8 electrodes for neonates as the space for electrodes placement is limited. In adults up to 32 electrodes are used. The frequency range of the AC current injected in typical EIT system is between 10 kHz to 1 MHz. EIT systems are classified in two types: passive and active. Active electrodes have electronic front end circuitry embedded in them. The active electrode (AE) [3] systems offer advantages over passive one in terms of performance and signal to noise ratio. However, in some applications, as in clinical ICUs to treat SARS-CoV-2 patients, the only viable option is the use of passive electrodes (PE). AE with their integrated electronics are not cost effective as they need to be replaced and disposed of on a regular basis.

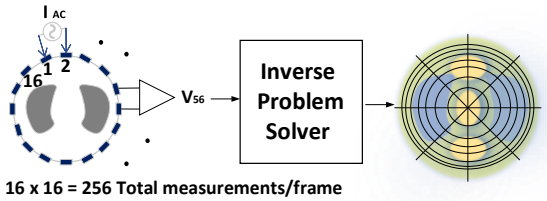

Fig. 1. EIT System.

In this paper a passive 16-electrode system is introduced that has direct applications in regional lung monitoring in the treatment of SARS-CoV-2 and neonatal patients. After this introductory part, section II describes the system architecture. Measured results are presented in section III while a suitable conclusion is drawn in section IV.

II. System Implementation

A. Overall Architecture

In the PE EIT system implemented, there are no active electronics at the point of contact to the subject under test (SUT). The SUT is connected to the EIT system using a cable and electrode belt made of textile/fabric with printed electrodes. The belt, printed electrodes and gel are made of biologically compatible materials. Fig. 2 shows the overall architecture used in the PE 16-electrode EIT system. The analogue front-end consists of two main parts: the driving ac

*Research supported by United Kingdom Research and Innovation (UKRI), grant No: EP/V044036/1

M. Rahal, J. Dai and Y. W, A. Demosthenous are all with the Department of Electronic and Electrical Engineering, University College London, London, UK, WC1E 7JE, (correspondence e-mail: m.rahal@ucl.ac.uk).

A. Bardill and R. Bayford are with the Department of Natural Sciences, Middlesex University, London, UK.

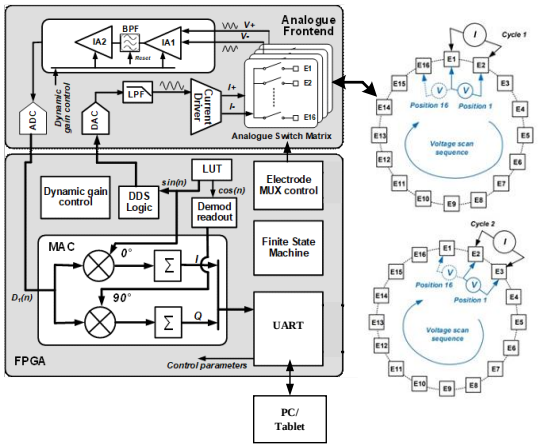

Fig. 2. Overall architecture.

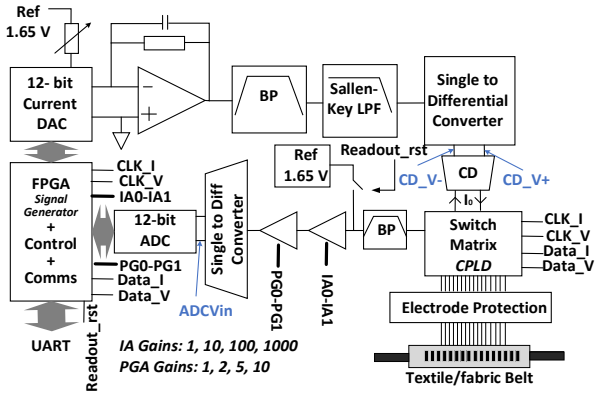

Fig. 3. Current drive and readout blocks.

current block and the readout circuitry. A *field programmable gate* array (FPGA) is used for control, waveform generation, digital demodulation, and *universal asynchronous receiver-transmitter* (UART) communications with a tablet. The interface between the FPGA and analog front-end is implemented using 12-bit data converters. A *complex programmable logic device* (CPLD) is used for switching to connect the current driver (CD) to the appropriate electrode pair and connecting the remaining electrodes to the readout part of the system. The overall system is powered through voltage regulators supplied from +/- 12 V, 5 V medically approved power supply. The PE system developed has a printed circuit board (PCB) footprint of 86.94 mm x 118.38 mm. The EIT box and connections to the belt and tablet are designed to comply with IP65 (*Protected from total dust ingress*) standard required in clinical applications in ICUs.

The control of the device is implemented using a finite state machine on the CMOD A7 FPGA. A lookup table is used to derive the sinusoidal signals needed to drive the current sources/sinks and in-phase and quadrature (I/Q) demodulation of the readout values. Dynamic gain control is implemented to ensure that readout values cover the analogue to digital converter range. Also, injection and readout patterns are fully programmable using the FPGA and CPLD (XC2C256-7VQ100I). The analogue to digital interface is implemented using two chips, 12-bit analogue to digital converter AD9237 ADC and 12-bit digital to analogue converter AD5445 DAC. The USB-UART data rate has been set to 5 Mbps, and it is used for both downlink and uplink data transfer.

There are 256 measurements in each frame, consisting of voltage measurements for 16 positions of current injection, where 16 voltage measurements were taken for each position of current injection. In cycle 1, current injection is at electrodes E1 and E2. Voltage measurement is taken first from E1 and E2, then shifts around the electrodes clockwise by one electrode at a time, until electrodes E16 and E1. In cycle 2 where current injection is at electrode E2 and E3, voltage measurement starts from E2 and E3, and finishes at electrodes E1 and E2. In summary, voltage measurement in each cycle always starts at the current injection electrodes. The result from each voltage measurement consists of 8 bytes, where the highest 4 bytes are the calculated real part of the measured voltage, and the lowest 4 bytes are the imaginary part. The values for both the real and imaginary parts are in a 32-bit 2's compliment format.

B. *Analog Front-End*

Fig. 3 shows a detailed implementation of the analogue front-end. The AD5445 current DAC is converted to voltage using a transimpedance amplifier AD8056. The band-pass filter followed by a low pass Sallen-key filter is implemented with a cut-off frequency of 1.7 MHz to smooth the sinusoidal signal before it is applied to the current driver. A single to differential converter with a gain of 2 is used to drive the fully differential current driver with a gain of 2 mA/V. The current amplitude can be varied by changing the reference voltage applied to the DAC. The supply rails of the current driver are set to +/- 5V to drive the electrodes at a wide range of frequency and controlled current levels. The CD can generate fully differential ac sinewave currents for frequencies up to 1 MHz with a maximum peak-to-peak amplitude of 13.3 mA.

The readout circuitry consists of several stages. The first stage is a high-pass filter to remove any offsets from the switching stage. This stage is followed by a low-noise instrumentation amplifier (IA) AD8253 stage with programmable gain (1, 10, 100 and 1000). The output of the IA is bandpass filtered to remove amplifier offset and reduce noise. A reset signal is applied before each voltage measurement is taken with the output connected and referenced to 1.65 V. The following stage is a programmable gain amplifier (PGA) AD8250 (1, 2, 5 and 10). The output of the amplifier is applied to a single-to differential AD8132 with a gain of 2. The differential outputs are fed to the ADC AD9237 with a sampling rate of 32 MSps set by the FPGA. CLK_I, CLK_V, DATA_I and DATA_V signals control the switch matrix for current injection and voltage scan patterns. The period of CLK_I is 16 times the period of CLK_V. The period of CLK_I is set to 512 µs allowing frame rate of up to 122 fps. The gains of IA and PGA can be adjusted automatically at the beginning of each voltage scan to increase the dynamic range before the output of the PGA is fed to the ADC. The reason is that the electrodes close to the injecting electrodes produce large signals compared to electrodes away from the injecting pair.

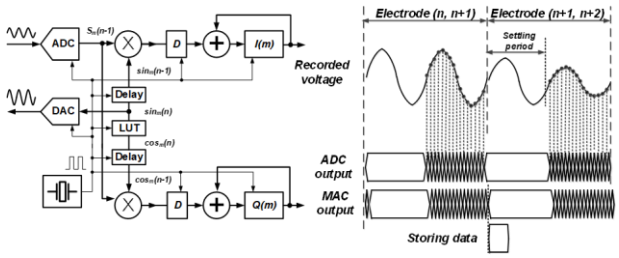

Fig.4. MAC architecture.

C. Data Acquisition and Data Representation

The FPGA performs I/Q demodulation to calculate the real and imaginary parts of the electrode voltage. The process is illustrated in Fig. 4. For each voltage measurement, the amplified electrode voltage is sampled at 32 MSps and then is digitized by a 12-bit ADC. High sampling rate is required to change the injection frequency in multi-frequency EIT systems. The input dynamic range of the ADC is 4V, which is evenly divided into 2^{12} intervals, giving a step size of digitization is $4/2^{12}$. A sampled amplified output is converted into an integer multiple of this step size, and the integer number is the digitization outcome, which is between -2048 and 2047. The real and imaginary components in the measurement voltage are calculated using digital I/Q demodulation where 512 digitized samples are each multiplied by a sample from prestored sine and cosine sequences, and then the products are accumulated. Since the prestored sine sequence is also used to generate the excitation signal. Therefore, the prestored sine sequence is in phase with the excitation current, neglecting the phase delay in the analogue front-end. The prestored sine and cosine sequence comprises of 12-bit samples of single frequency sine and cosine waves, respectively, so an ideal sine wave between -1 and 1 is presented by a digital sequence between -2048 and 2047. The calculated real and imaginary components of each measurement, V_I and V_Q, according to the process illustrated in Figure 4, can be written as:

$$V_I = \frac{1}{N}\sum_{n=0}^{N-1} V_{ADC}(n).floor(2^{11}.sin\frac{2\pi n}{N/m}) \quad (1)$$

$$V_Q = \frac{1}{N}\sum_{n=0}^{N-1} V_{ADC}(n).floor(2^{11}.cos\frac{2\pi n}{N/m}) \quad (2)$$

where N=512 and *floor()* is a function for rounding the value to the closest smaller integer, and m is the total number of cycles of the voltage signal sampled in a predefined window. Since the sampling window per measurement is fixed at 16 µs and the sampling frequency is fixed at 32 MSps, the 512 samples cover different number of cycles of the excitation signal depending on the excitation frequency. The value m is 2 for 125 kHz, 4 for 250 kHz, 8 for 500 kHz and 16 for 1 MHz. The $V_{ADC}(n)$ is the digitized voltage is given by

$$V_{ADC}(n) \times \frac{4V}{2^{12}} = V_{electrode}(n) \times 2 \times Set\_gain \quad (3)$$

where $V_{electrode(n)}$ is the sampled voltage on the electrodes before being amplified. The amplifiers have a fixed gain of 2 and a dynamic gain, *Set_gain*, set by the software.

III. Measured Results

Fig.5 shows the measured differential inputs to the current driver with 125 kHz injection. With a CD gain of 2 mA/V this differential swing can produce a 4 mApp current to drive the electrodes.

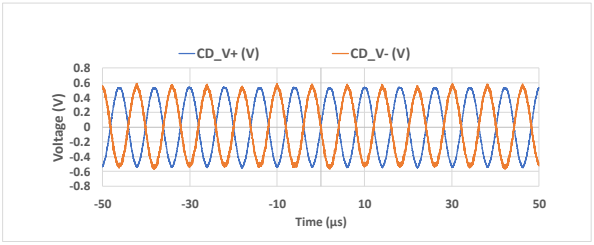

Fig.5. Measured current driver signals (CD_V+, CD_V-) for 125 kHz injection. With differential amplitude of 2 Vpp giving a current of 4 mApp.

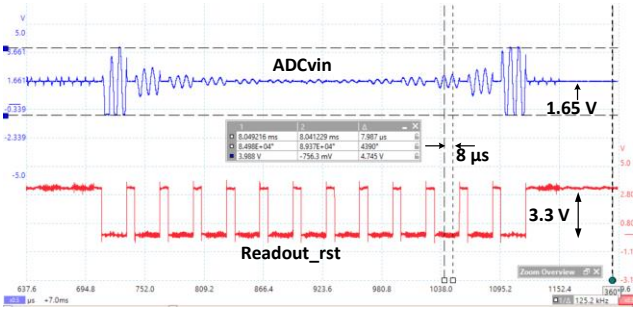

Fig. 6. ADC input and Readout_rst with fixed gain for IA (100) and PGA (10). 4 mApp current at 125 kHz is injected at electrodes.

In order the assess the system performance, measured results were obtained using a resistive phantom [4]. Fig. 6 shows the ADC input with Readout_rst signals applied when 4 mApp current injection is applied at 125 kHz to the resistive phantom. Fixed gain values for IA and PGA were set to 100 and 10, respectively. 13 segments of the recording are shown excluding the remaining 3 segments that involve the two injecting electrodes. The voltage scan gave higher amplitude where the recording electrodes are close to the injection electrodes, and lower amplitudes where the recording electrodes are further away from the injection site. The recordings of segments 1 and 13 saturated the amplification stage, whereas the middle segments gave a very low signal level causing a significant degradation to the signal to noise ratio and therefore to the quality of the EIT image. Fig. 7 shows the input to the ADC and Readout_rst when gain control is applied to the IA and PGA. No saturation is observed for electrodes close to the injection electrodes and in addition, the middle segments are significantly amplified to fit the range of the ADC. To assess the noise performance and its effect on the EIT image quality, a *full reference* (FR) method is used [4]. Low values of the FR metric indicate close matching with the reference image. Figure 8 shows the noise performance of the PE EIT system with fixed gains of IA and PGA, 100 and 10, respectively. Figure 8a) shows the reference image generated by a reconstruction algorithm based on difference imaging with respect to the reference image by using GREIT [5]. The simulated image shows two *regions of interests (ROI) with* different resistivities compared to the rest of the image. Blue areas represent high resistivity, whereas red areas represent low resistivity. Fig. 8b) represents the image generated from the PE EIT system with fixed gains for IA and PGA of 100 and 10, respectively. 50 frames were collected from the resistive phantom for comparison with the reference image. Fig. 8c) shows the global FR in the image compared to the reference

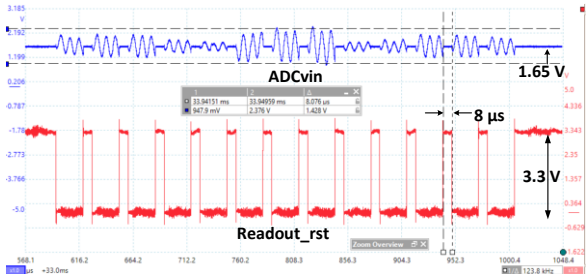

Fig.7. ADC input and Readout_rst with variable gains for IA and PGA. 4 mApp current at 125 kHz is injected at electrodes.

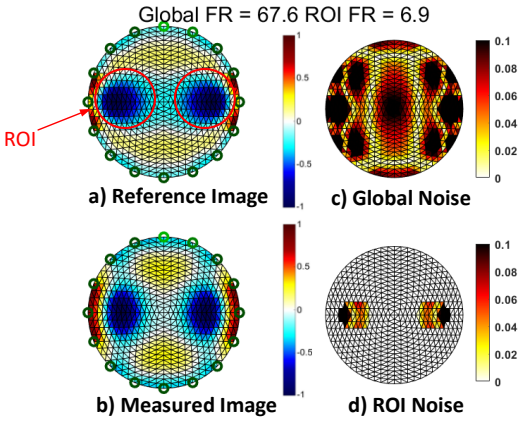

Fig.8. Noise performance with fixed gains. A) reference image, b) measured image with fixed gains of IA (100) and PGA (10), c) global noise and d) ROI noise. 4 mApp current at 125 kHz is injected at electrodes.

image, whereas in Fig. 8d) the FR of the ROI is shown. Choosing fixed gains in the PE EIT system has a major impact on the EIT image generated. Fig. 9 shows the performance of the EIT system with controlled gains for IA and PGA. Significant reductions in FR metrics are obtained. The ROI FR metric showed a reduction of 70% compared to the case with fixed gains for IA and PGA. Table I outlines the main specifications of the PE EIT system. In addition, comparison with other EIT systems is given.

IV. Conclusion

In this paper, a PE EIT system is introduced that has the potential to be applied in applications for the monitoring of regional lung ventilation for SARS-CoV-2 and neonatal patients. The system is compact on one single double-sided PCB and consumes 1.7 W of power. The system can run at a frame rate of 89 fps and its gain settings are automatically adjusted to increase the dynamic range and improve the accuracy of the EIT image. The EIT system is designed to comply with IP65 (*Protected from total dust ingress*) standard required in clinical applications in ICUs.

References

[1] Y. Wu, D. Jiang, A. Bardill, S. De Gelidi, R. Bayford, and A. Demosthenous, "A high frame rate wearable EIT system using active electrode ASICs for lung respiration and heart rate monitoring," *IEEE Trans.Circuits Syst. I Regular Papers*, vol. 65, no. 11, pp. 3810–3820, Nov. 2018.

[2] A. Romsauerova, A.McEwan, L. Horesh, R.Yerworth, R. H. Bayford, and D. S. Holder, "Multi-frequency electrical impedance tomography (EIT) of the adult human head: Initial findings in brain tumours, arteriovenous malformations and chronic stroke, development of an analysis method and calibration," Physiol. Meas., vol. 27, no. 5, pp. S147–161, 2006.

[3] Y.Wu , D. Jiang, A. Bardill, R. Bayford and A. Demosthenous, " A 122 fps, 1MHz Bandwidth multi-frequency wearale EIT belt featuring novel active electrode architecture for neonatal thorax vital signs monitoring," IEEE Trans. Biomed. Circuits Syst, vol. 13, no. 5, pp. 927-937, Oct. 2019.

[4] Y. Wu, D. Jiang, Rebecca Yerworth and A. Demosthenous, "An image Based Method for Universal Peformance Ealuation of Electrical Impedance Tomography Systems," IEE Trans. Biomed. Circuits Syst, vol. 15, no. 3, pp.464-473, June. 2021.

[5] A. Adler, J. Arnold , R. Bayford , A. Borsic, B. Brown, P. Dixon, T. Faes, I. Frerichs , H. Gagnon, Y. Gärber , B. Grychtol , G. Hahn, W. Lionheart, A. Malik , R. Patterson , J. Stocks, A. Tizzard , N. Weiler and G. Wolf, "GREIT: a unified approach to 2D linear EIT reconstruction of lung images," *Physiol. Meas.*, vol. 30, no. 6, pp., S35-S55, 2009.

[6] "Swisstom BB^2", (2015). [online] Available: https://fdocuments.in/document/product-brochure-swisstom-bb2-english-version-pdf-18-mb.html.

[7] "Dräger PulmoVista® 500 ICU Ventilation and Respiratory Monitoring", [online] Available: https://www.draeger.com/Products/Content/pulmovista-500-pi-9066475-en-master-1911-1.pdf.

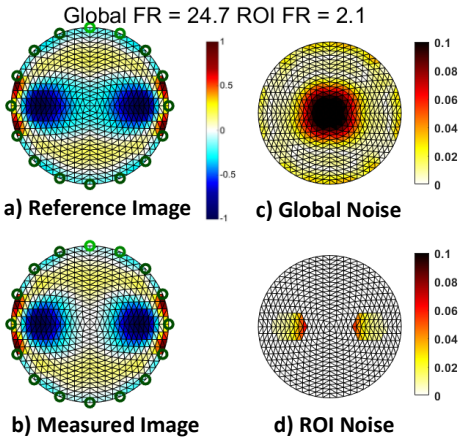

Fig.9. Noise performance with controlled gains. A) reference image, b) measured image, c) global noise and d) ROI noise. 4 mApp current at 125 kHz is injected at electrodes.

TABLE I. PE EIT System Specifcation

Feature	*This work*	*Swisstom [6]*	*Dräger PulmoVista ® 500 [7]*
Number of electrodes	16	32	16
Belt	Fabric	Ref. electrode	
Frame Rate (fps)	**89**	50	<=30
Frequency (kHz)	125-1000	150	80 to 130
Supp. Voltage (V)	+/- 12, 5	Mains supply	
Power Cons. (W)	**1.7**	60	80
Current Amp. (mA)	Up to 6.65	IEC60601-1	IEC60601-1
Prog. Pattern	Yes		
Elect/Contact Measurement	Yes		
Comms. Interface	UART storage	USB /Ethernet	USB